

Phenomena of Nanotube Formation on the Surface of Cp-Ti, Ti-6Al-4V, and Ti-Ta alloys

K. Lee, *H.C. Choe, Y.M. Ko, ¹W. A. Brantley

College of Dentistry, Chosun University, 2nd stage of Brain Korea 21 for College of Dentistry,
Gwangju, Korea

¹College of Dentistry, Ohio State University, Columbus, OH, USA
[*hcchoe@chosun.ac.kr](mailto:hcchoe@chosun.ac.kr)

ABSTRACT

In this study, the phenomena of nanotube formation on the surface of Ti alloys by electrochemical method. Nanotube layer formed on Ti alloys in 1 M H₃PO₄ electrolyte with small additions of F⁻ ions. The pore growth behavior was clearly different on individually phase and was also different for alloys. On the α -phase of Cp-Ti and β -phase of Ti-30Ta alloy, the nanotube showed clearly highly ordered TiO₂ layer. In case Ti-30Ta alloy, the pore size of nanotube was smaller than of Cp-Ti due to β stabilizing Ta element. In this case of Ti-6Al-4V alloy, the α phase showed stable porous structure; the β -phase was dissolved entirely.

Keywords: Nano-structure, Ti-Ta alloy, dental implant

1 INTRODUCTION

Commercial pure titanium(Cp-Ti) and Ti-6Al-4V are widely used as a dental root implant material in clinical dentistry and as orthopedic implant material because of its mechanical strength, stability, and good compatibility with bone tissue[1-3]. This high degree of biocompatibility is thought to be due to the titanium surface forming a stable oxide layer(TiO₂ matrix) that presumably aid in the formation of an osteogenic extracellular matrix at the implant-bone tissue interface, which is important for osseointegration[4-5]. Recently published experimental studies seem to indicate that on nanotube formation, a nanotube of the thickness of the native oxide, will result in very strong reinforcement of the bone response. Webster et al.[6] reported that on nanograined ceramics such as alumina oxide and titanium oxide (~100 nm regime), improved bioactivity of implant and enhanced osteoblast adhesion are observed. Since the appearance of the first report on formation of nanoporous anodic oxide film of Ti and Ti-6Al-4V alloy in 1999 by Zwilling et al.[7], a significant number of reports is available on the anodization of Ti in different fluoride solutions [8-10]. Synthesis of homogeneously ordered straight forward because of a single phase microstructure, however, show a dual phase α + β

microstructure. The α -phase, which has a hcp structure, is enriched with hcp stabilizing element such as Al, oxygen, nitrogen, etc.; whereas β -phase, with a bcc structure, is enriched with beta-stabilizing elements such as V, Nb, Mo, Ta, etc. because of the difference in chemistries of these phases, the formation of the nanotubular oxide layer was not uniform in the Ti alloys having dual phase microstructure as one phase could get etched preferentially by the electrolyte. Tsuchiya et al. [11] anodized Ti-28Nb-13Ta-4.6Zr alloy in two different microstructural conditions and observed uniform presence of ordered oxide nanotubes when the microstructure was a single β -phase. In the dual phase (α + β) condition, the oxide layer was not uniform and contained nano-scratches and etched pore wall.

In this study, the phenomena of nanotube formation on the surface of Ti alloys by electrochemical method. Nanotube layer formed on Ti alloys in 1 M H₃PO₄ electrolyte with small additions of F⁻ ions. The pore growth behavior was clearly different on individually phase and was also different for alloys. On the α -phase of Cp-Ti and β -phase of Ti-30Ta alloy, the nanotube showed clearly highly ordered TiO₂ layer.

2 MATERIALS AND METHODS

2.1 Alloy preparation

Titanium and the following titanium alloys were studied: Ti-6Al-4V and Ti-30Ta (the numbers signify the wt.%). They were manufactured by arc melting on a water-sealed copper hearth under an argon gas atmosphere with a non-consumable tungsten electrode. Each ingot was melted six times by inverting the metal to ensure homogeneous melting. Fig. 1 shows the heating condition for Ti alloys. Cp-Ti and Ti-30Ta alloy were homogenized in argon atmosphere at 1000°C (which is above the β transus temperature) for 24h followed by a rapid quenching in ice water. Ti-6Al-4V was carried out at 1000°C for 12h. After water quenching the Ti-6Al-4V were aged at 560°C for 2h and water quenching. They cut to a diameter of 10 mm and a thickness of 2 mm followed by diamond cutter. Prior to anodizing, polished

sample were etched (the mixture of HNO₃ and HF aqueous solution) to remove the surface oxidized, followed by ultra sonic cleaning in acetone for approximately 10 min.

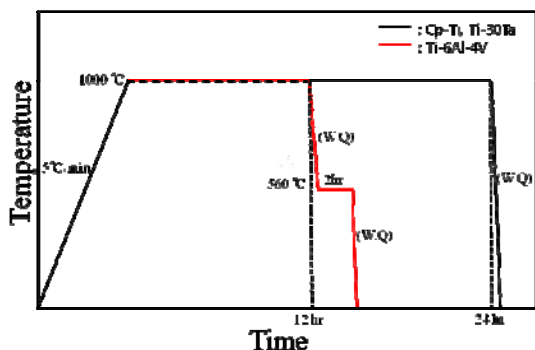


Figure 1: Schematic diagram to illustrate the heating condition for the Ti alloys

2.2 Anodization treatments

Electrochemical experiments were carried out with conventional three-electrode configuration with a platinum counter electrode and a saturated calomel reference electrode. The sample was embedded with epoxy resin, leaving a square surface area of 10 mm² exposed to the anodizing electrolyte, 1 M H₃PO₄ containing 0.64 wt.% NaF. Anodization treatments were carried out using a scanning potentiostat (EG&G Co., Model 362, USA). All experiments were conducted at room temperature. The electrochemical treatments consist of potential was first swept from the open-circuit potential to desired final potential with a sweep rate of 500 mV/s, then the potential was held for 2h. After the treatments the anodized sample were rinsed with distilled water and dried with dry air stream.

2.3 Material characterization

The microstructures of the studied alloys were investigated by optical microscope (OM, Olympus BM60M) and scanning electron microscope (Hitachi S-3000). The samples for the OM and SEM analysis were etched in Keller's solution. In order to identified the phase constitutions of Ti alloys, X-ray diffraction (XRD, X-pert Pro) analysis with a Cu-K α radiation were performed.

Structural characterization of the anodized samples was carried out with a field emission scanning electron microscope (FE-SEM, Hitachi S-4800). The scanning electron microscope was capable of energy dispersive spectrometer(EDS, Oxford).

3 RESULT AND DISCUSSION

3.1 Microstructural observations

Fig. 1 shows the optical microstructures of Cp-Ti, Ti-6Al-4V and Ti-30Ta alloys. It controlled by heat treatment in Ar atmosphere followed by 0°C water quenched. It exhibits martensite structure, and Cp-Ti alloy was acicular structure of α -phase, Ti-6Al-4V alloy was lamellar structure of α + β phase and Ti-30Ta alloy was needle-like structure of β -phase.

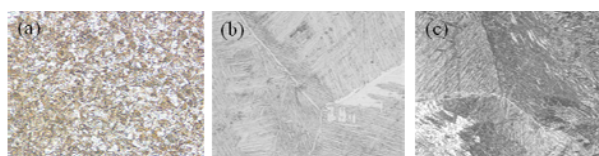


Figure 2 : OM micrographs showing the microstructure of heat treated Ti alloys ($\times 200$) . (a) Cp-Ti, (b) Ti-6Al-4V, (c) Ti-30Ta

Fig. 2 show the SEM image and EDS result of Cp-Ti, Ti-6Al-4V and Ti-30Ta alloys. It can be seen that acicular, lamellar and needle-like structure, respectively. As a result of EDS, chemical composition was in accord with alloys design.

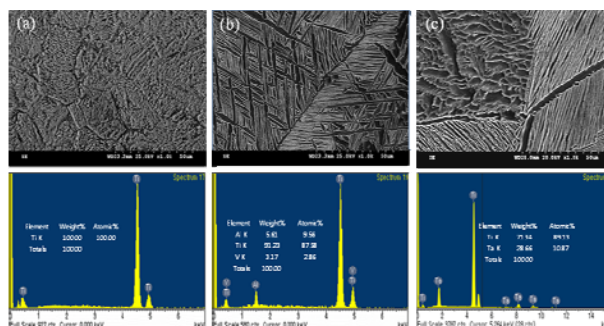


Figure 2 : SEM micrographs and EDS results of heat treated Ti alloys (a) Cp-Ti, (b) Ti-6Al-4V, (c) Ti-30Ta

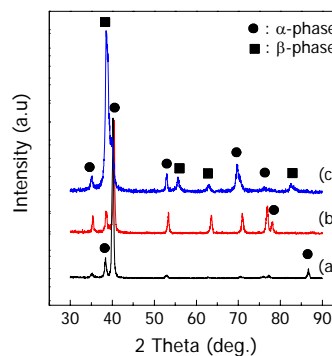


Figure 3: XRD diffraction patterns of heat treated Ti alloys (a) Cp-Ti, (b) Ti-6Al-4V, (c) Ti-30Ta

Fig. 3 shows the X-ray diffraction profiles of Cp-Ti, Ti-6Al-4V and Ti-30Ta alloys. The peaks were indexed using the JCPDS diffraction data of Ti-alloys. Cp-Ti alloy and Ti-30Ta alloy can be seen that only reflections from α and β phase, respectively. And Ti-6Al-4V alloy was identified $\alpha+\beta$ phase. Ti-30Ta alloy has the beta phase in XRD peaks.

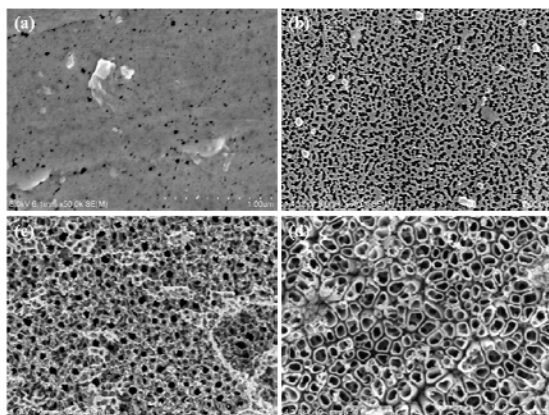


Figure 4: FE-SEM images of the anodic porous oxide layers formed at final voltage after periods of potential sweep : (a) 0 min, (b) 30 min, (c) 60 min, (d) 120 min

Fig. 4 shows FE-SEM images of the anodic porous oxide layers formed at final voltage after periods of potential sweep. Nanotube diameter increased predominantly as anodized time increased. The nuclei of nanotube on Cp-Ti surface is very small in case of anodizing time for 30min as shown in Fig. 4(b), whereas, in the case of anodizing time for 120min, nanotube diameter size is about 100nm. It is confirmed that nanotube of diameter and depth depend on anodizing time.

Fig. 5 shows (a) top and (b) cross-section of anodized on Cp-Ti surface. The clear nanotube structures with large diameter have been formed on Cp-Ti compared to other specimen. The nanotubes of Cp-Ti have an inner average diameter of 80~100 nm with a tube-wall thickness of about 20nm. Ti-6Al-4V alloy shows stable porous nanotube formation in the only α -phase structures, whereas, sponge-like structure was formed in β -phase.

The nanotube size formed on β -phase of Ti-30Ta surface has smaller porous than that of nanotube formed Cp-Ti surface on α -phase surface. It can be concluded that it is not easy to dissolve oxide film for nanotube formation due to formation of Ta oxide like Ta_2O_5 on the passive film.(Fig 5a, b).

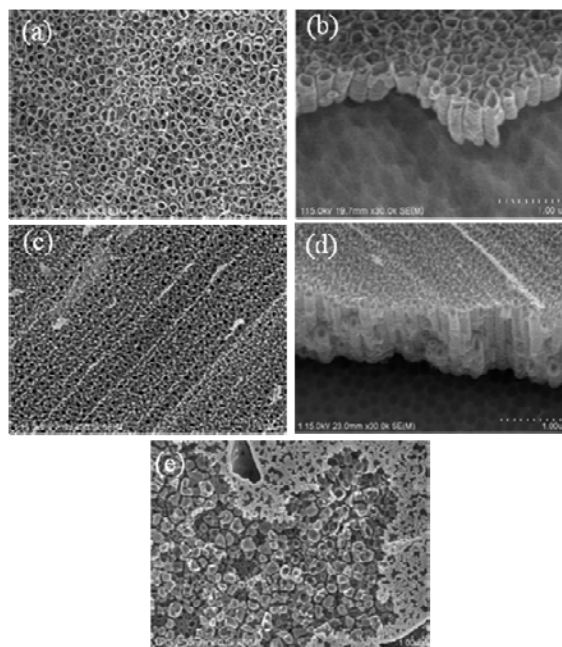


Figure 5: FE-SEM images of nanotube layers formed at different phase of Ti alloys (a) Cp-Ti top-view, (b) Cp-Ti cross-section, (c) Ti-30Ta top-view, (d) Ti-30Ta cross-section, (e) Ti-6Al-4V top-view

4 CONCLUSIONS

1. From the microstructure analysis, Cp-Ti showed acicular structure of α -phase, Ti-6Al-4V showed lamellar structure of $\alpha+\beta$ phase and Ti-30Ta showed needle-like structure of β -phase.
2. As a result of EDX, chemical composition was in accord with alloys design. Cp-Ti, Ti-6Al-4V, and Ti-30Ta alloys, individually α , $\alpha+\beta$ and β were identified by XRD.
3. The nuclei of nanotube on Cp-Ti surface is very small in case of anodizing time for 30min whereas, in the case of anodizing time for 120min, nanotube diameter size is about 100nm. Therefore nanotube of diameter and depth depend on anodizing time.
4. The nanotubes of Cp-Ti have an inner average diameter of 80~100 nm with a tube-wall thickness of about 20nm. Ti-6Al-4V alloy shows stable porous nanotube formation in the only α -phase structures, whereas, sponge-like structure was formed in β -phase. The nanotube size formed on β -phase of Ti-30Ta surface has smaller porous than that of nanotube formed

ACKNOWLEDGEMENT

“This work was supported by research funds from Chosun University (2007) and 2nd stage of Brain Korea 21 for College of Dentistry”

REFERENCES

- [1] A. Schoeder, F. Sutter, G. Krekeler, Oral implantology. Newyork : Thieme Medical, 35-58, 1991
- [2] T. Albrektsson, P. I. Branemark, H. A. Hansson, K. Kasemo, K. Larsson. I. Loundstrom, D.H. McQueen, R. Skalak, "The interface zone of inorganic implants *in vivo* : Titanium implants in bone" Ann Biomed Eng, 11, 21-27, 1983
- [3] D.F. Williams, "Titanium and titanium alloys : Biocompatibility of clinical implant materials", Boca Raton, FL:CRC Press, Vol 1, 9-44
- [4] B. Kasemo, J. Lausmaa, "Biomaterial and implant surface : a surface scienc approach" Int J Oral Maxillofac Implant, 3, 247-259
- [5] C.M. Stanford, J. C. Keller, "Osseoinetergration and matrix production at the implant surface" Crt Rev Oral Biol Med 2, 83-101, 1991
- [6] T. J. Webster, C. Ergun, R. H. Doremus, R.W. Siegel, R. Bizios, "Enhanced functions of osteoblasts on nano-phase ceramics", 21, 1803-1810, 2000
- [7] V. Zwillling, E. Darque-Ceretti, A. Bountry-Forveille, D. David, M. Y. Perrin, M. Acounturier, "Structure and Physicochemistry of Anodic oxide Films on Titanium and TA6V Alloy", Surf Interface Anal, 27, 629-637, 1999
- [8] G. K. Mor, O. K. Varghes, M. Paulose, K. Shankar, C. A. Grines, "A review on highly ordered, vertically oriented TiO₂ nanotube arrays: Fabrication, material properties, and solar energy applications", Sol. Energy Mater Sol Cells, 90, 2011-2075
- [9] S. P. Albu, A. Ghicov, J. M. Macak, P. Schmuki. "250 μm long anodic TiO₂ nanotubes with hexagonal self-ordering" Phys Stat Sol, 1, R65-R67, 2007
- [10] K. S. Raja, T. Gandhi, M. Misra," Effect of water content of ethylene glycol as electrolyte for synthesis of ordered titania nanotubes", Electrochem Commun, 9, 1069-1076, 2007
- [11] H. Tsuchiya, J. M. Macak, A. Chicov, Y. C. Tang, S. Fusimoto, M. Niinomi, T. Noda, P. Schmuki, "Nanotube oxide coating on Ti-29Nb-13Ta-4.6Zr alloy prepared by self-organizing anodization", Electrochim Acta, 52, 94-101, 2006